Journal of Applied Mechanics and Technical Physics, Vol. 45, No. 1, pp. 133–141, 2004

MODELING OF THE FRONT OF MELTING AND DESTRUCTION OF A MELT FILM DURING GAS-LASER CUTTING OF METALS

O. B. Kovalev, A. M. Orishich, A. P. Petrov, V. M. Fomin, P. V. Yudin, A. N. Malov, and G. V. Ermolaev

UDC 621.373.826

The products of laser cutting of metals on an automated laser setup are investigated. Results of model experiments are presented, where soft wax was used instead of metal transforming into the melt; soft wax filled a narrow flat slot between two glass plates and was removed by a heated air stream. The physical processes of melting of the liquid-wax film, its destruction, and entrainment by the gas jet being assumed to be analogous to the processes of metal-melt spraying inside the cut in full-scale experiments, the characteristic size of drops formed thereby is evaluated. The modeling results are in qualitative agreement with the results of full-scale experiments. It is shown that the quality of laser cutting of metals directly depends on the character of spraying of the liquid melt and the process of its removal.

Key words: *laser cutting, metal, melting, gas jet, motion of a liquid film, destruction of the liquid, roughness, burr, modeling.*

Introduction. Advanced CO_2 lasers are widely used in laser treatment of materials (drilling, welding, and cutting). Engineering achievements in this field are limited and are applicable only to articles of small thickness made of some types of ferrous metals (low-carbon steel, stainless steel, and electrotechnical steel). The character of interaction of laser radiation with metals depends on the laser power, reflective and absorptive properties of metals, and thermophysical properties of the latter. It is assumed that light energy is absorbed in metals in a thin surface layer by electrons transferring their energy to the lattice during collisions, which results in metal heating.

Gas-laser cutting is performed by means of local melting of the metal and removal of the melt by the gas jet. Laser cutting can be performed with immediate evaporation of the metal [1]. In this case, however, one needs a laser with a high density of incident radiation (greater than 10^{10} W/m^2) and with blowing to ensure removal of metal vapors. For iron, the melting heat is $H_{\rm melt} = 277$ kJ/kg, which is much smaller than the evaporation heat $H_{\rm boil} = 6340$ kJ/kg. Therefore, a more economical method, which does not require high laser power is gas-laser cutting, in which the metal is locally (within the spot of focused radiation) heated to the melting point and is entrained due to intense blowing of the gas jet.

The main aspects of gas-laser cutting of materials are presented in [1, 2]; the existing concepts on the laser-beam structure, the character of its interaction with the surface, and the cutting mechanism are described. Comparative characteristics of the current technologies of laser cutting with the use of CO_2 lasers, Nd : YAG lasers, and excimer lasers are presented. Criteria characterizing the quality of cutting by various laser systems are described. The issues of diagnostics, optimization, and quality control are discussed. A physical model of melt removal from the cut by the gas flow and formation of regular roughness is proposed in [3]. Quantitative estimates of cut defects (roughness and burr) and results of experimental studies of cutting of electrotechnical steel samples are presented in [3, 4]. The quality of laser cutting is characterized by the cut width, deviation of the side surfaces of the cut from the perpendicular direction to the sheet plane, magnitude of surface roughness, and absence or presence of burrs (solidified drops of the melt on the lower surface of the cut). Kovalev et al. [5] analyzed the physical processes

Institute of Theoretical and Applied Mechanics, Siberian Division, Russian Academy of Sciences, Novosibirsk 630090. Translated from Prikladnaya Mekhanika i Tekhnicheskaya Fizika, Vol. 45, No. 1, pp. 162–172, January–February, 2004. Original article submitted June 30, 2003.

Fig. 1. Formation of burrs on the back side of the cut during gas-laser cutting of an electrotechnical steel sheet (sheet thickness $h = 0.5$ mm, laser power $W = 800$ W, cutting velocity $U = 9$ m/min, pressure $p = 0.6$ MPa, working gas is nitrogen).

observed in gas-laser cutting of metals and formulated the problems of their mathematical simulation. It is noted that gas-laser cutting of metals includes a large number of interrelated physical processes: supersonic channel-slot flow of the gas; unstable flow of the liquid film of the melt with formation of waves on the liquid surface, which are caused by the force action of the gas; heat transfer due to heat conduction in the solid metal with a moving spatial boundary; formation of burrs and roughness bands on the side surfaces.

The description of the processes is hindered by the necessity of taking into account a large number of physical parameters (thermophysical properties of the material, parameters of the gas jet, cutting velocity, plate thickness, and radiation parameters). Proper cutting velocity, jet parameters, and radiation parameters should be chosen to provide optimal high-quality cutting. Kovalev et al. [5] suggested an optimal approach where the generic statement of the problem is formulated mathematically in the form of adjoint subproblems of mechanics of continuous media with moving boundaries. Under certain simplifying assumptions, one can solve these subproblems analytically. As a result, an estimate was obtained for the thickness of the liquid melt film and dynamics of its growing over the cut depth as a function of the cutting velocity. One of the reasons for formation of burrs and regular roughness on the side surfaces is the unsteady motion of the melt film. At the moment, there are only some hypothetical concepts on the character of melt film motion inside the cut under the action of the gas jet. An attempt to experimentally study the interaction of the gas jet with the liquid melt film inside a narrow channel is made in the present work.

Results of Full-Scale Experiments. To obtain experimental data on cutting quality and the size of particles formed in the products of gas-laser cutting, the study was performed on an automated laser setup with a laser power up to 5 kW. Radiation similar to the TEM_{00} mode was focused by a lens with a focal distance $F = 190$ mm onto the surface of the material being cut. The diameter of the radiation spot in the caustic surface of the lens was about 150–200 μm. Figure 1 shows the photograph of burrs arising when the cutter motion regime changes near the corner, where deceleration and a decrease in velocity occur. Figure 2 shows typical "strokes" (regular roughness) arising on the cut surface.

The experiments show that, during gas-laser cutting of steel sheets of thickness $h \geqslant 5$ mm, melt removal is accompanied by bright fluorescence of the finest melted particles in the two-phase gas jet issuing from the cut being formed. If the two-phase jet contains small particles of the condensed phase, the cut quality is satisfactory. If the particles are large and the exhaustion has the character of oscillations with periodic outburst of large drops or melt blobs, the cut quality is poor (burrs, roughness bands, etc.). Thus, the cut quality directly depends on the character of melt spraying and removal. Figure 3 shows the photographs of condensed phase particles sampled in the two-phase jet. The size distribution of particles is plotted in Fig. 4. One can see that almost all particles have a spherical shape, and their size decreases with decreasing cutting velocity and radiation power. Most particles have sizes within 80–150 μm, which is significantly smaller (sometimes, severalfold smaller) than the cut width.

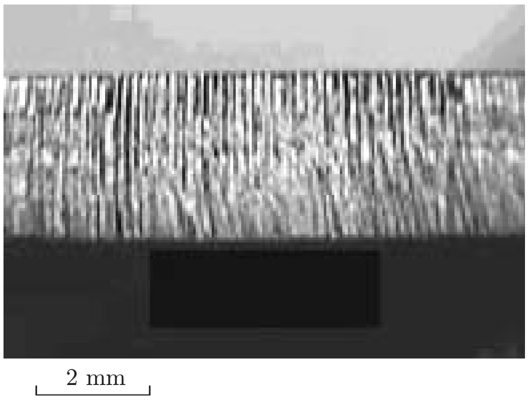

Fig. 2. Roughness bands on the side edge of the cut obtained during gas-laser cutting of a low-carbon steel sheet ($h = 4$ mm, $W = 900$ W, and $U = 1.7$ m/min; working gas is oxygen).

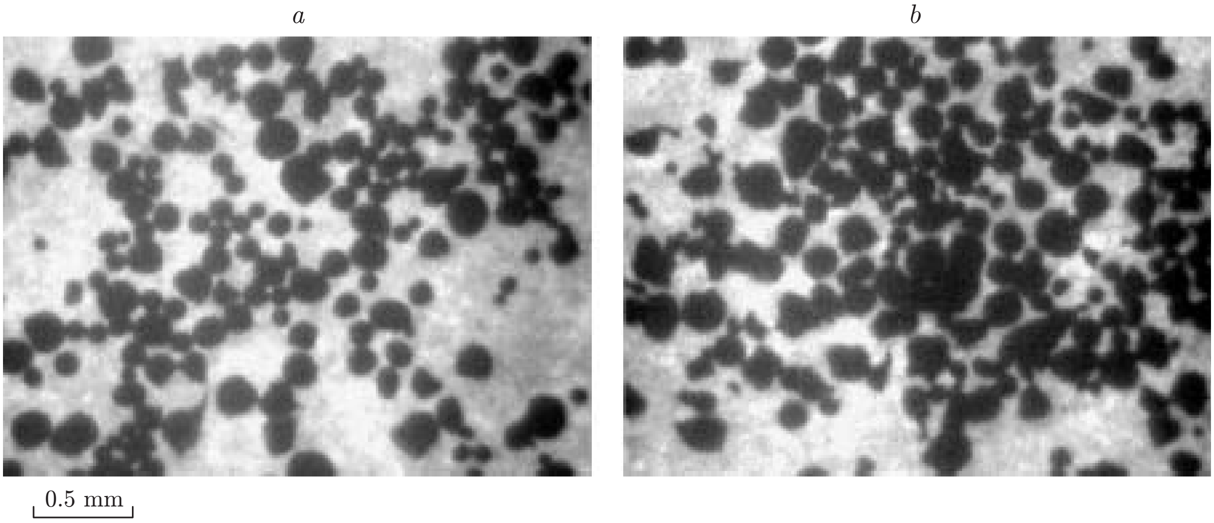

Fig. 3. Condensed phase particles entrained from the cut by the two-phase jet in the full-scale experiment with the use of the laser setup in the case of gas-laser cutting of a stainless steel sheet ($h = 2$ mm, $p = 0.8$ MPa, and $W = 2.5$ kW): $U = 3$ (a) and 4 m/min (b).

Results of Model Experiments. The local character of radiation, high thermal loads, and small cut width make it rather difficult to visualize the processes of melt formation and removal from the cut in full-scale experiments on gas-laser cutting of metals. To study the interaction of the gas jet with the melt in a narrow channel, we performed special experiments on a model setup whose sketch is shown in Fig. 5. Air from a gas holder through an electric heater was fed to a nozzle unit similar to a gas-laser cutter. The air jet issued from a confuser nozzle mounted directly above a slot 1 mm wide between two extended glass plates, which was filled by solidified wax. The model was displaced by the MP-100 mechanism with a certain velocity, whereas the position of the nozzle above the slot remained unchanged. The role of the liquid metal was performed by wax, which melted upon interaction with the air jet heated up to a temperature above 100°C and was ejected from the slot. This process was registered by a video camera, and the video signal was fed into the PC memory. The filming was performed in reflected light from an ISh-5 pulse lamp triggered by a power source with the filming frequency. The moments of flashes were determined by frame synchropulses identified from the video signal by the synchronization unit.

According to [6], wax is a crystalline substance, which is a mixture of saturated hydrocarbons with a melting point of about 50°C. The thermophysical properties of wax [6] and stainless steel [7] are listed in Table 1. The melting pattern of wax depends on the model-displacement velocity and parameters of the hot air jet. Figures 6–8 show the frames taken with an interval of 0.125 sec, which show the dynamics of the wax melting front under

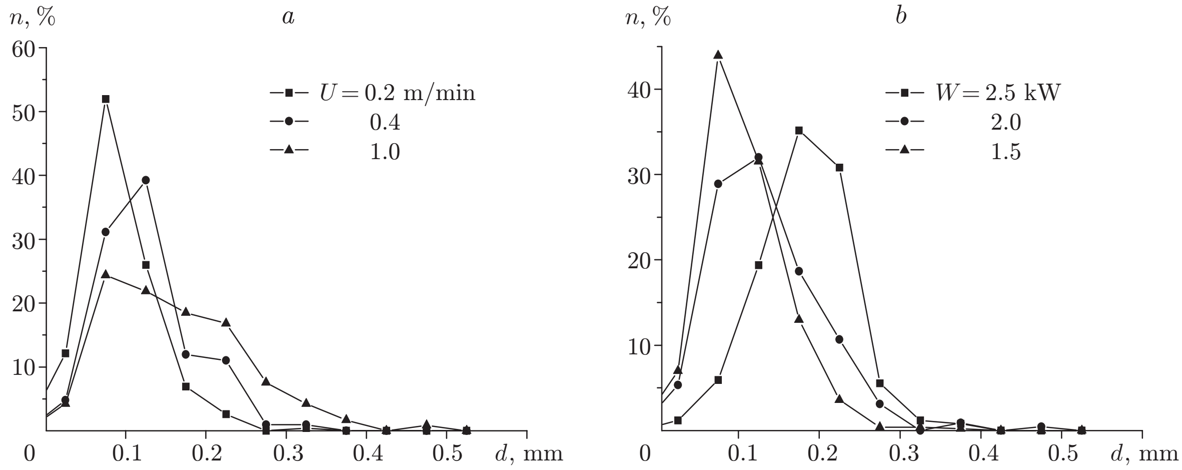

Fig. 4. Size distribution of the condensed phase particles for different cutting conditions: (a) $h = 3$ mm, $W = 2.5$ kW, and $p = 1.1$ MPa; (b) $h = 2$ mm, $U = 3$ m/min, and $p = 0.8$ MPa.

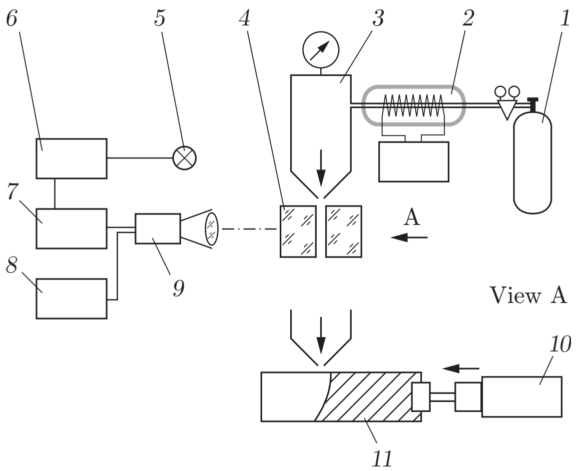

Fig. 5. Sketch of the model setup: 1) gas holder with compressed air; 2) electric heater; 3) model of the nozzle unit of the laser cutter; 4) glass plate; 5) ISh-5 pulse lamp; 6) power source for the lamp; 7) synchronization unit; 8) computer; 9) video camera; 10) drive for MP-100; 11) wax.

different conditions and also the specific features of the flow and destruction of the melt film. When the air pressure in the nozzle chamber is low (about 0.3 MPa), the melt-film flow is accompanied by formation of waves on the liquid surface (Fig. 6). As the pressure increases to 0.5 MPa, a step arises on the melting front, and liquid shedding with formation of single droplets occurs (Fig. 7). With further increase in pressure (up to 0.7 MPa), the step shifted toward the cut output increases, and destruction of the liquid wax film in the spraying regime in the form of a wide band is observed (Fig. 8).

Models of Liquid Film Destruction and Droplet Formation. It is assumed in [3, 4] that the melt is formed under the action of a moving laser beam and flows at the cut front in the form of a thin film entrained by the gas flow. The regular structure of roughness is formed due to periodic shedding of melt droplets by the gas flow from the upper edge of the cut front. These droplets, initially retained by capillary forces, are shed under the action of the pressure gradient at the entrance to the cut and slide down the thin melt film. To estimate the size of the formed droplets, Makashov et al. [3] proposed the formula

$$d = 2(\sigma d_{\text{beam}}(1 - \text{M}^2)/(p\gamma \text{M}^2))^{1/2}, \qquad \text{M} < 1. \tag{1}$$

Here d is the droplet diameter, σ is the surface tension of the liquid melt, d_{beam} is the beam diameter, M is the Mach number in the gas, p is the gas pressure, and γ is the ratio of specific heats. In the model of [3], it is not

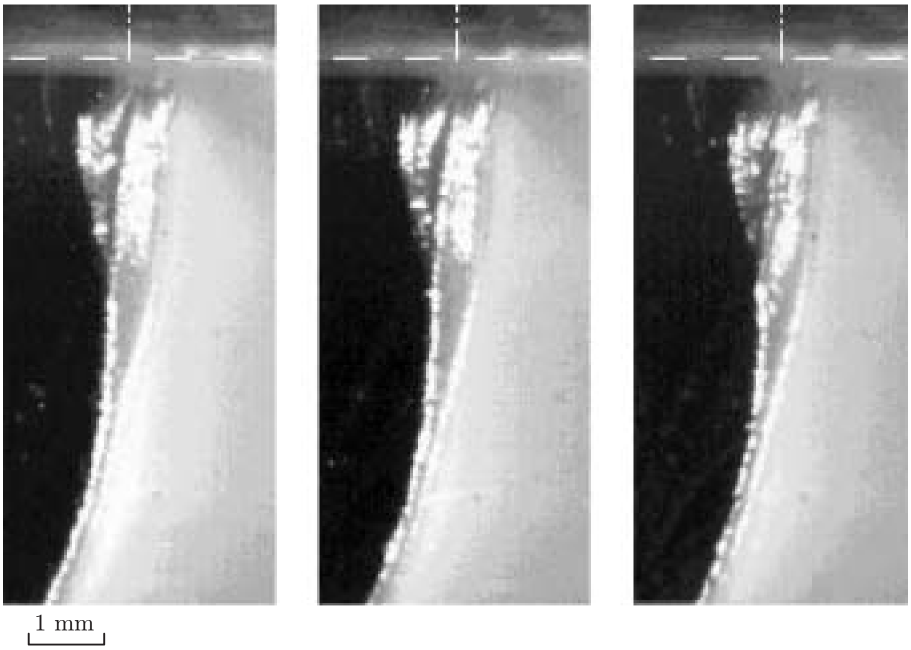

Fig. 6. Frames with an interval of 0.125 sec from the initial stage of wax melting with formation of waves on the surface of a thin melt film flowing down under the action of hot air: the light and dark regions refer to solid wax and air stream, respectively; the dot-and-dashed line is the nozzle centerline, and the dashed line is the upper boundary of the glass plates.

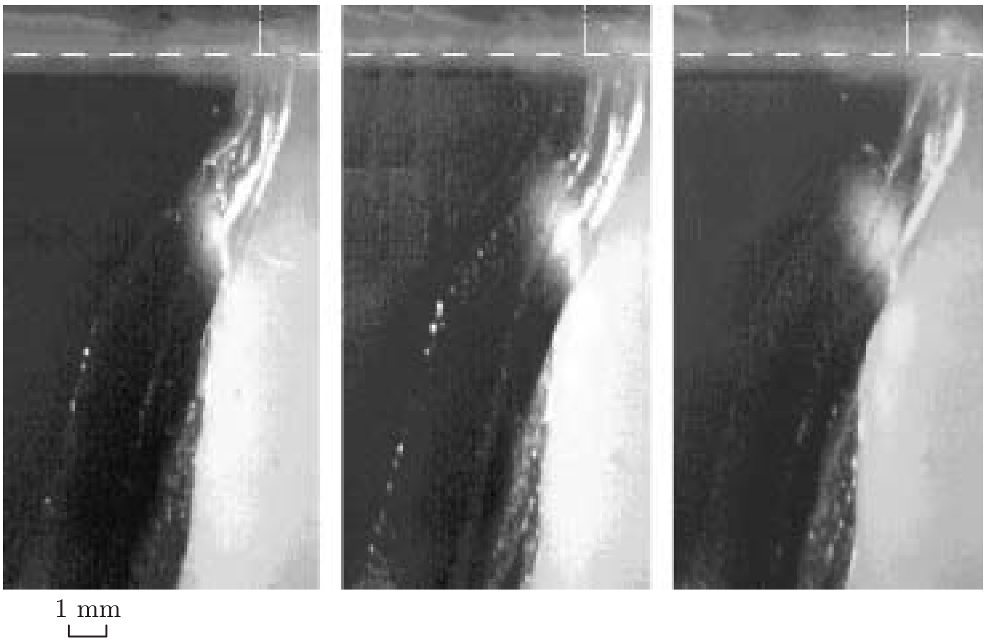

Fig. 7. Frames of destruction of the liquid wax film and formation of droplets (the interval between the frames and the legend are the same as in Fig. 6).

TABLE 1

Parameter	Material	
	Wax [6]	Stainless steel AISI 304 [6, 7]
ρ_s, kg/m^3	900	6900 (1397°C), 6610 (1727°C)
c_p, kJ/(kg · K)	1.58 (−20–3°C), 2.98 (60°C)	0.477 (17°C), 0.707 (1397°C), 0.810 (1457°C)
λ_s, W/(m · K)	0.123 (30°C)	31.5
$\mu_{\text{liq}} \cdot 10^3$, N/(sec · m^2)	4.0 (40°C), 2.6 (60°C), 1.8 (80°C), 1.4 (100°C), 1.09 (150°C)	2.8 (1397°C)
σ, N/m	0.0404	1.87*, 0.9**
T_{liq}, °C	54	1397
H_{liq}, kJ/kg	147	272
k_{liq}, m^2/sec	$4.6 \cdot 10^{-8}$	$5.68 \cdot 10^{-6}$

Notes. The temperature at which the given value of the material parameter was obtained is given in brackets; the values of σ in vacuum and air are marked by one and two asterisks, respectively.

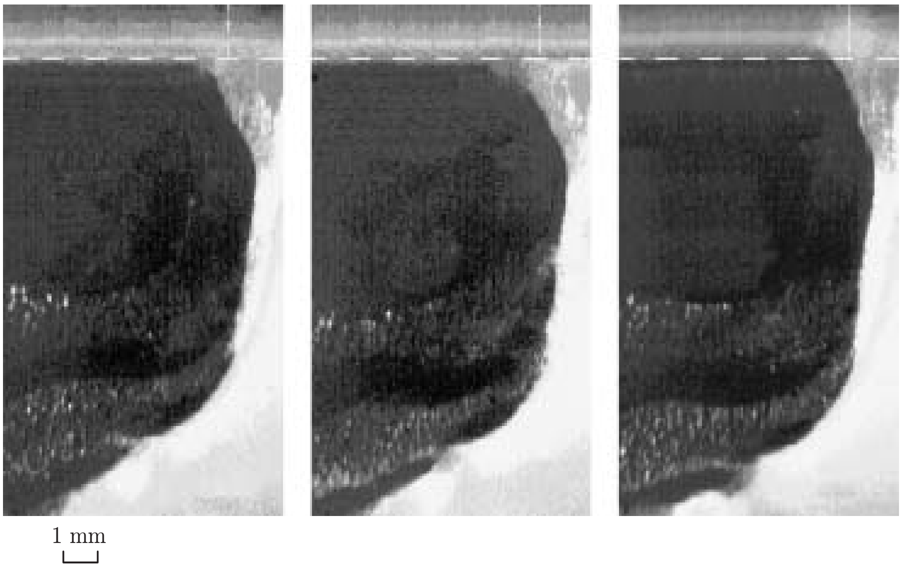

Fig. 8. Frames of destruction of the liquid wax film in the spraying mode (the interval between the frames and the legend are the same as in Fig. 6).

assumed that destruction of the liquid melt and droplet formation can occur inside the cut. Formula (1) was not verified experimentally.

The problem of spraying of liquid films by the gas jet and prediction of the size of droplets shed from the film surface still remains important, extremely complicated, and defying rigorous description. Flow stability and destruction of liquid films have been considered in a large number of papers (see [8, 9] and the bibliography therein).

The characteristics of film flow and its destruction depend on many parameters. Internal reasons for instability are various initial perturbations that cause origination of waves on the surface. Such waves are usually called capillary waves [10]. External reasons for instability are caused by the action of aerodynamic forces on the film surface; the values of these forces depend on the velocity of film motion and density and velocity of the cocurrent gas flow. Such waves are called acceleration waves [11]. The aerodynamic forces tend to deform and break the film, whereas liquid viscosity prevents this process. The method of small perturbations widely used in mechanics for solving problems of stability of liquid film motion [9, 12, 13] does not allow one to reliably evaluate the size of the droplets being formed. In studying liquid fragmentation in the gas flow, the Weber criterion is often used: $\text{We} = \rho_{\text{g}}(V_{\text{g}} - V_p)d/\sigma$, where ρ_{g} and V_{g} are the gas density and velocity, σ is the surface tension of the liquid, and V_p and d are the droplet velocity and diameter.

On the basis of [15], Levich [14] obtained the following formula for estimating the droplet size in the absence of shock waves for liquid spraying in pneumatic injectors:

$$d = \chi\Big(\frac{1}{V_{\rm g}}\sqrt{\frac{\sigma}{\rho_{\rm liq}}}\Big)^{1.2} L^{0.4}\Big(\frac{\rho_{\rm liq}}{\rho_{\rm g}}\Big)^{0.2}. \quad (2)$$

Here, d [μm] is the diameter, χ is the dimensionless empirical coefficient whose value in [16] was assumed to be equal to 12, $V_{\rm g}$ [m/sec] is the air velocity, σ [N/m] is the surface tension, $\rho_{\rm liq}$ [kg/m^3] is the liquid density, $\rho_{\rm g}$ [kg/m^3] is the gas density, and L [m] is the maximum possible scale of turbulent oscillations equal to the width or diameter of the narrow cross section of the gas channel. It is noted in [16] that the experimental results on fragmentation of liquids by spraying injectors disagreed with the calculated values in terms of the Weber criterion.

According to [17], Eq. (2) allows one to evaluate the Sauter mean diameter of droplets shed from the surface of the liquid film exposed to a cocurrent gas flow. The experiments of [17] were performed under a pressure close to atmospheric on a setup that had the form of a horizontal plate exposed to an air jet parallel to the plate surface with three values of jet velocity: $V_{\rm g} = 30$, 42, and 62 m/sec. Water was injected onto the plate from a flat slot 0.5 mm wide. The Sauter mean diameter of the droplet was determined by the formula $d = \sum n_i d_i^3 / \sum n_i d_i^2$, where d_i is the current diameter of the droplet and n_i is the number of droplets of diameter d_i. It is shown in [17] that the experimental values of d are in good agreement with those calculated by formula (2), where the value of the coefficient χ was assumed to be 8.5.

Let us consider two possible regimes of liquid film destruction in a narrow channel of the cut in more detail on the basis of the filming frames shown in Figs. 6–8. The first regime is observed if waves whose amplitude is comparable to the film thickness arise on the liquid surface (see Fig. 6). As long as the surface of the solid–liquid phase transition remains smooth, the film is not destroyed. Destruction is observed when inhomogeneities in the form of upward or downward steps appear on the solid surface. The film in the form of a jet is shed from the step and instantaneously decomposes into droplets of approximately identical size, moving one behind the other along the same trajectory, being entrained by the gas flow (see Fig. 7). The second regime is observed when the force action of the gas increases with increasing pressure. In this regime, droplets of different diameters are shed from the liquid surface, and film destruction proceeds in the spraying mode (see Fig. 8).

We assume that film destruction and droplet formation occur due to origination of waves on the liquid surface. Let us consider acceleration waves [11] caused by aerodynamic drag forces. The influence of capillary forces (arising due to surface tension) is ignored, since their contribution to energy is insignificant as compared to acceleration waves. The wave amplitude on the film surface by the moment of shedding is assumed to be comparable to the film thickness. Formation of spherical droplets of approximately identical size, moving along the same trajectory (see Fig. 3), occurs at the moment of film shedding; hence, the volume of each droplet is one half of the volume of the body obtained by rotating the cosine wave around the axis passing through its minimums. The volume is $v = \pi \int_{-\lambda/2}^{\lambda/2} y^2\,dx = 0.5\pi\lambda A^2$ [$y = A\cos(\pi x/\lambda)$ is the cosine wave equation; A and λ are the wave amplitude and wave length]. If we assume that the volume of the droplets being formed is equal to one half of the volume v, the relation $\pi d^3/6 = 0.25\pi\lambda A^2$ readily yields the droplet diameter $d = (1.5\lambda A^2)^{1/3}$. According to [10], the time evolution of the amplitude of the wave formed on the liquid surface under the action of a permanently acting aerodynamic force is described by the equation

$$\frac{dA}{dt} = A\Big(\frac{\pi\beta\rho_{\rm g}(V_{\rm g} - V_{\rm liq})^2}{\lambda\rho_{\rm liq}V_{\rm liq}} - \frac{8\pi^2\mu_{\rm liq}}{\rho_{\rm liq}\lambda^2}\Big),$$

where $0 < \beta \leqslant 1$ is the windage parameter, $V_{\rm liq}$ and $\mu_{\rm liq}$ are the liquid velocity and liquid viscosity, respectively, and t is the time. The critical value of the wavelength $\lambda_{\rm cr}$ of the most rapidly growing perturbation is determined from the condition $dA/dt = 0$. As a result, we obtain $\lambda_{\rm cr} = 8\pi\mu_{\rm liq}V_{\rm liq}/(\beta\rho_{\rm g}(V_{\rm g} - V_{\rm liq})^2)$. The wave amplitude A should be related to film thickness. If we assume that $A = k_1 h$ (h is the mean thickness of the melt film and $1 < k_1 < 2$ is a parameter), we obtain the following formula for the droplet diameter:

$$d = \Big(\frac{12\pi k_1^2}{\beta}\,\frac{\mu_{\rm liq}V_{\rm liq}h^2}{\rho_{\rm g}(V_{\rm g} - V_{\rm liq})^2}\Big)^{1/3}. \quad (3)$$

Calculation Results. The results calculated by formulas (1)–(3) are listed in Table 2. It should be noted that formulas (1)–(3) differ not only in structure but also in physical parameters entering into them.

TABLE 2

Formula	Values of parameters	d, μm
$d = 2\left(\dfrac{\sigma d_{\text{beam}}(1-\text{M}^2)}{p\gamma \text{M}^2}\right)^{1/2}$	$\sigma = 0.95$ N/m, $d_{\text{beam}} = 700$ μm, M $= 0.54$, $p = 0.88$ MPa, $\gamma = 1.4$	62.6
$d = \chi\left(\dfrac{1}{V_{\text{g}}}\sqrt{\dfrac{\sigma}{\rho_{\text{liq}}}}\right)^{1.2} L^{0.4}\left(\dfrac{\rho_{\text{liq}}}{\rho_{\text{g}}}\right)^{0.2}$	$\chi = 8.5$, $V_{\text{g}} = 187$ m/sec, $\sigma = 0.95$ N/m, $\rho_{\text{liq}} = 6610$ kg/m^3, $L = d_{\text{beam}} = 700$ μm, $\rho_{\text{g}} = 10.6$ kg/m^3	15.6
$d = \left(\dfrac{12\pi k_1^2}{\beta}\,\dfrac{\mu_{\text{liq}} V_{\text{liq}} h^2}{\rho_{\text{g}}(V_{\text{g}} - V_{\text{liq}})^2}\right)^{1/3}$	$\beta = 0.5$, $k_1 = 1.8$, $\mu_{\text{liq}} = 2.8 \cdot 10^{-3}$ N/(sec $\cdot$ m^2), $V_{\text{liq}} = 60$ m/sec, $V_{\text{g}} = 187$ m/sec, $\rho_{\text{g}} = 10.6$ kg/m^3, $h = 60$ μm	107.0

The characteristic diameter of single droplets formed in the upper part of the cut front and then sliding down over the melt film is found by Eq. (1). Radiation power and properties of the melt film are ignored in Eq. (1). The resultant value $d = 62.6$ μm differs from the mean size of droplets in full-scale experiments (see Fig. 3).

The empirical formula (2) yields an estimate of the size of droplets shed from the film itself (from wave ridges); therefore, the values of the droplet diameter are very low ($d = 15.6$ μm). Formula (2) can be used to calculate the mean diameter of droplets formed in the film spraying mode.

Finally, formula (3) takes into account many factors; the main of them are the gas parameters (ρ_{g} and V_{g}) and the liquid parameters (μ_{liq}); it is especially important that this formula takes indirectly into account the radiation parameters and the cutting velocity, which affect the velocity V_{liq} and thickness h of the liquid film. The value $d = 107$ μm is in satisfactory agreement with the results of full-scale experiments. It is suggested that formula (3) should be used to evaluate film destruction in the regime of single particles.

The gas density and velocity in the slot and the liquid film velocity and thickness were calculated by the method of [5].

Justification of Model Experiments. Gas-laser cutting of metals involves a large set of complicated interrelated physical processes; therefore, it does not seem possible to study this process as a whole.

The objective of the present work was to perform a model experiment to study the interaction of a gas jet with a liquid melt of a material inside a narrow channel geometrically similar to a laser cut. For this purpose, the facility layout (Fig. 5) was developed under the following considerations. We had to create conditions with possible interaction of three phases, where the material would pass from the solid state to the liquid state with a clear phase-transition boundary and be mechanically destroyed by the gas jet. The geometric characteristics of the slotted cut and injector, as well as the gas-jet parameters were in complete agreement with the full-scale facility. The process of jet–liquid interaction inside the cut was visualized through glass walls. Glass is known to be destroyed under the action of a laser beam. By replacing metal by soft wax, however, one can reduce the thermal load on the system by providing heat for wax melting by a hot air jet. It should be taken into account that the jet not only penetrates into the slot but also interacts with glass. Nevertheless, the low thermal conductivity of glass and wax localizes heat addition to a certain extent, similar to the laser beam. Physical characteristics of wax are significantly different from characteristics of metals almost in all aspects (see Table 1); therefore, it is impossible to reach complete similarity of the processes in wax and metal. It can be assumed, however, that still there is some partial similarity. Results of mathematical simulation of gas-laser cutting of metals are reported in [5]. Equations written in a dimensionless form contain the Prandtl, Stefan, and Peclet numbers, and other dimensionless complexes. With a proper choice of the cut velocity and width, one can obtain identical Peclet numbers, which ensures almost complete similarity of temperature distributions. In this case, the thicknesses of the melt layer differ by a factor of 1.5–2. Formula (2) involves the ratios of parameters σ/ρ_{liq} and $\rho_{\text{liq}}/\rho_{\text{g}}$ (moreover, the latter ratio is raised to the small power of 0.2), and the calculated values of d for metal and wax differ only by a factor of 3 for identical velocity and density of the gas. Thus, we have $d = 15.6$ μm for metal and $d = 5.2$ μm for wax (see Table 1).

Comments and Conclusions. It is shown experimentally that the quality of laser cutting directly depends on the character of liquid spraying by the gas jet.

Melting and formation of the liquid melt of the material in a narrow channel and its removal by the gas jet as applied to gas-laser cutting of metals are visualized. It is shown that melt removal is accompanied by destruction of the liquid film and formation of droplets whose size depends on liquid properties, film thickness, and gas-jet parameters. Destruction of the liquid film occurs inside the cut in the regime of formation of single particles due to film shedding from the step and in the regime of spraying into numerous small droplets, which are entrained by the gas in the flow core and do not interact with channel walls.

Analytical dependences are proposed for calculating and estimating the droplet size. Formulas (2) and (3) can be considered as "point" formulas, i.e., they are satisfied at each point of the liquid–gas interface, which allows one to use these formulas for numerical simulation of hydro-gas-dynamic flows in the channel of the cut.

Further development of the considered method of simulation implies that the properties of the model material should be brought closer to metal properties, which would allow optimization of actual cutting of metals.

The authors are grateful to V. B. Shulyat'ev for discussion of results and useful comments.

REFERENCES

1. J. Pawell, CO_2 *Laser Cutting*, Springer-Verlag (1993).
2. A. Gropp, J. Hutfless, S. Schuberth, and M. Geiger, "Laser beam cutting (invited paper)," *Optic. Quant. Electron.*, **27**, 1257–1271 (1995).
3. N. K. Makashov, E. S. Asmolov, V. V. Blinkov, et al., "Gas dynamics of cutting metals by continuous laser radiation in an inert gas," *Kvant. Élektron.*, **19**, No. 9, 910–915 (1992).
4. V. I. Ledenev, V. A. Karasev, and V. P. Yakunin, "Relation of capillary phenomena and defect formation during gas-laser separation of metals," *Izv. Ross. Akad. Nauk, Ser. Fiz.*, **63**, No. 10, 2047–2052 (1999).
5. O. B. Kovalev, A. M. Orishich, V. M. Fomin, and V. B. Shulyat'ev, "Adjoint problems of mechanics of continuous media in gas-laser cutting of metals," *J. Appl. Mech. Tech. Phys.*, **42**, No. 6, 1014–1022 (2001).
6. I. K. Kikoin (ed.), *Tables of Physical Quantities: Handbook* [in Russian], Atomizdat, Moscow (1976).
7. P. Strömbeck and A. Kar, "Self-focusing and beam attenuation in laser materials processing," *J. Phys., D, Appl. Phys.*, **31**, 1438–1448 (1998).
8. Yu. F. Dityakin, L. A. Klyachko, B. V. Novikov, et al., *Spraying of Liquids* [in Russian], Mashinostroenie, Moscow (1977).
9. V. E. Nakoryakov, B. G. Pokusaev, and I. R. Shraiber, *Propagation of Waves in Gas– and Vapor–Liquid Media* [in Russian], Inst. Thermophysics, Novosibirsk (1983).
10. H. Lamb, *Hydrodynamics*, Cambridge Univ. Press (1932).
11. M. Adelberg, "Mean drop size resulting from the injection of a liquid jet into a high-speed gas stream," *AIAA J.*, **6**, 1143–1147 (1968).
12. M. Vicanek, G. Simon, H. M. Urbassek, and I. Decker, "Hydrodynamical instability of melt flow in laser cutting," *J. Phys., D, Appl. Phys.*, **20**, 140–145 (1987).
13. A. J. Babchin, A. L. Frenkel, V. G. Levich, and G. I. Sivashinsky, "Nonlinear saturation of Rayleigh–Taylor instability in thin films," *Phys. Fluids*, **26**, No. 11, 3159, 3160 (1983).
14. V. G. Levich, *Physicochemical Hydrodynamics* [in Russian], Fizmatgiz, Moscow (1959).
15. A. N. Kolmogorov, "Fragmentation of droplets in a turbulent flow," *Dokl. Akad. Nauk SSSR*, **66**, No. 5, 825–828 (1949).
16. R. M. Yablonik and É. É. Markovich, "Structure of the formula for the mean size of droplets in a pneumatic injector," *Izv. Vys. Uch. Zaved., Énergetika*, No. 6, 72–74 (1966).
17. É. É. Markovich, V. V. Guguchkin, and N. I. Vasil'ev, "Parameters of droplets shed from a liquid film," Cherkassy (1988). Deposited at Krasnodar Polytech. Inst. on 06.05.87, No. 484-KhP-87.